Inorg. Chem. **2006**, *45*, 2713–2717

$Ae_2Sb_2X_4F_2$ (Ae = Sr, Ba): New Members of the Homologous Series $Ae_2M_{1+n}X_{3+n}F_2$ Designed from Rock Salt and Fluorite 2D Building Blocks

Houria Kabbour and Laurent Cario*

Institut des Matériaux Jean Rouxel, CNRS−Université de Nantes, 2 rue de la Houssinière, 44322 Nantes Cedex 1, France

Received November 14, 2005

We have designed new compounds within the homologous series $Ae_2F_2M_{1+n}X_{3+n}$ (Ae = Sr, Ba; M = main group metal; n = integer) built up from the stacking of 2D building blocks of rock salt and fluorite types. By incrementally increasing the size of the rock salt 2D building blocks, we have obtained two new $n = 1$ members of this homologous series, namely, $Sr_2F_2Sb_2Se_4$ and $Ba_2F_2Sb_2Se_4$. We then succeeded in synthesizing these compounds using a high-temperature ceramic method. The structure refinements from the powder or single-crystal X-ray diffraction data confirmed presence of the expected alternating stacking of fluorite [Ae_2F_2] (Ae = Sr, Ba) and rock salt [Sb_2Se_4] 2D building blocks. However the Ba derivative shows a strong distortion of the [Sb_2Se_4] block and a concomitant change of the Sb atom coordination likely related to the lone-pair activity.

Introduction

The past twenty years have seen the development of the concepts of secondary building units (SBU) and self-assembly that gave most supramolecular chemists the ability to design new compounds. More recently, these concepts were successfully transferred to the design of new hybrid compounds. In contrast, the crystal engineering of inorganic compounds that do not contain an organic part remains a challenging task. Because of the lack of reliable ab initio structure prediction methods, it is indeed still rare that the synthesis of a new pure inorganic compound targets a predicted composition and structure. But, as pointed out by Mackoviky and co-workers, the modular description of crystal structures combined with phase homologies could provide an elegant alternative method to predict the structures of such compounds.[1] Indeed, most complex atomic arrangements can be described using one, two, or more modules that are fragments of archetypal structures. A series of structures sharing the same modules and the same building principles form a homologous series. The most recognized are likely the Aurivillius $Bi_2A_{n-1}B_nO_{3n+3}$ (A = alkaline, alkaline earth, rare earth, Bi, etc.; B = transition metal, etc.),[2] the Magnéli[3] or Dion-Jacobson $A[A'_{n-1}B_nO_{3n+1}]$ (A = alkaline, etc.; A′= Ca, Nd; B = Nb)[4−6] homologous series. A general formulation capturing the homology rules expresses the composition of all known members within the series by incrementally increasing the size of each module in various dimensions. This general formulation generates a large number of hypothetical compounds with predictable structures and compositions. Consequently, the identification of new homologous series has the power to partly meet the challenge of design of new pure inorganic compounds. Mrotzek and Kanatzidis have brilliantly illustrated this idea by identifying a new homologous series $A_m[M_{1+l}Se_{2+l}]_{2m}$-$[M_{2l+n}Se_{2+3l+n}]$ (A = alkali metal; M= main group IV and V element) based on two types of columnar rock salt modules cut out along different directions.[7] Homologies were first observed between a few compounds obtained by exploratory synthesis. Subsequently, systematization of the stoichiometries under a common general formulation helped in the design of a large number of new members by tuning the

* To whom correspondence should be addressed. Phone: 00 33 (0)2 40 37 39 48. E-mail: Laurent.Cario@cnrs-imn.fr.

(1) Ferraris, G.; Mackoviky, E.; Merlino, S. *Crystallography of Modular Materials*; Oxford University Press: New York, 2004.
(2) Aurivillius, B. *Ark. Kemi* **1949**, *1*, 463.
(3) Magnéli, A. *Acta Crystallogr.* **1953**, *6*, 495.
(4) Dion, M.; Ganne, M.; Tournoux, M. *Mater. Res. Bull.* **1981**, *16*, 1429−1435.
(5) Dion, M.; Ganne, M.; Tournoux, M.; Ravez, J. *Rev. Chim. Miner.* **1984**, *21*, 92−103.
(6) Jacobson, A. J.; Johnson, J. W.; Lewandowski, J. T. *Inorg. Chem.* **1985**, *24*, 3727.
(7) Mrotzek, A.; Kanatzidis, M. G. *Acc. Chem. Res.* **2003**, *36*, 111−119.

10.1021/ic051969x CCC: $33.50
Published on Web 02/18/2006

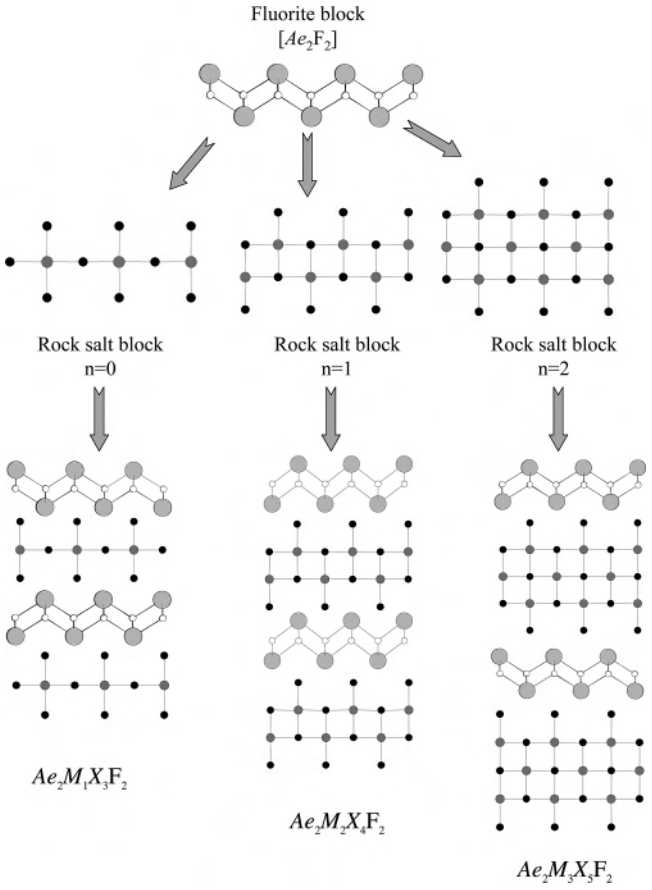

Figure 1. Representation of the structures of the first three members of the homologous series $Ae_2M_{1+n}X_{3+n}F_2$ (Ae = Sr, Ba; M = main group metal; X = S, Se; n= integer) built from the stacking of rock salt $[M_{1+n}X_{3+n}]$ and fluorite $[Ae_2F_2]$ 2D building blocks.

size of each module (i.e., by varying the three integer indices, n, l, and m).

In the particular case of infinite 2D modules, we have recently shown that the design of new pure inorganic compounds with 2D structural features required even less of a prerequisite.[8,9] The prediction of both the structures and the compositions of such compounds is attainable simply from the stacking of known 2D modules of distinct chemical natures, without the need to generalize a formulation from known compounds. For example, the structure of $Ba_2F_2SnS_3$ was predicted from the stacking of 2D building blocks of the rock salt and fluorite types.[10] Because the size of the rock salt 2D building blocks can easily be tuned, we could forecast a new homologous series $Ae_2M_{1+n}X_{3+n}F_2$ (Ae = Sr, Ba; M = main group metal; n= integer) with predictable structures (see Figure 1). Within this homologous series, $Ba_2F_2SnS_3$ represents the first member with $n = 0$, but to our knowledge, no higher homologues with n ≥ 1 are known so far.

This paper reports on the search for new members of the homologous series $Ae_2M_{1+n}X_{3+n}F_2$ (Ae = Sr, Ba; M = main group metal; n= integer). Considering the rock salt $[Sb_2Se_4]$ 2D building blocks, we could predict the structure of two new homologues with $n = 1$, namely, $Sr_2Sb_2Se_4F_2$ and $Ba_2Sb_2Se_4F_2$. This paper describes the synthesis, chemical characterization, and structure refinement of these compounds.

Experimental Section

Synthesis. Both compounds $Sr_2Sb_2Se_4F_2$ and $Ba_2Sb_2Se_4F_2$ were synthesized using a similar high-temperature ceramic method. For $Sr_2Sb_2Se_4F_2$, a stoichiometric proportion of SrF_2, SrSe, and Sb_2Se_3 was weighed and ground in an argon glovebox. The mixture was subsequently pressed into pellets and sealed under vacuum in a silica tube. The tube was first heated at a rate of 30 °C/h to 220 °C for a first step lasting 12 h, and then it was heated at 50 °C/h to 600 °C for a second step lasting 12 h. For $Ba_2Sb_2Se_4F_2$, we used BaF_2, Ba, Sb_2Se_3, and Se as the starting materials, and we heated the tube to 700 °C.

Chemical Analysis. The chemical analysis of both compounds was performed on powder samples or crystals using a scanning electron microscope JEOL 5800LV equipped with an additional EDX apparatus (energy-dispersive analysis of X-rays) IMIX-PGT with a germanium detector. The presence of fluorine was confirmed for both compounds but this element could not be quantified because of experimental limitations.

X-ray Powder Data Collection. The X-ray powder diffraction analysis of $Sr_2Sb_2Se_4F_2$ was performed on a D5000 diffractometer using the Cu Kα radiations ($\lambda K_{\alpha1}$ = 1.540598 Å and $\lambda K_{\alpha2}$ =1.54439 Å). The data collection was performed at room temperature in the 10−110° 2θ range with an acquisition time of 12 h. The cell parameters and the crystal structure refinements were performed by the Rietveld method using the programs FullProf [11] and WinPlotr.[12] The background was fitted by a linear interpolation between selected points. The March−Dollase model was used for preferred orientation along the (001) direction, and the pseudo-Voigt function was used as the peak-shape model.

X-ray Single-Crystal Data Collection and Structure Refinement. A single crystal of $Ba_2Sb_2Se_4F_2$ with a parallelepipedic shape (dimensions 0.035 × 0.060 × 0.100 mm^3) was mounted on a Nonius Kappa CCD diffractometer, using Mo Kα radiation (λ = 0.71073 Å). The crystal-to-detector distance was 35.0 mm; 472 frames were collected with a rotation angle per frame of 2° and an exposure time of 200 s. The diffraction pattern was consistent with the triclinic system. We could refine the unit cell parameter values: a = 6,1944(12) Å, b = 6,3315(13) Å, c = 13,804(3) Å, α = 85,34(3)°, β = 85,18(3)°, and γ = 89,82(3)°.

Intensities were corrected for absorption (μ = 25.70 mm^{-1}) using the face-indexed option. The structure was solved with the use of the direct methods (SHELXS), and refinements with subsequent difference Fourier were done with SHELXL.[13] The structure solution was easily obtained. In the final stage of refinement (i.e., with all atoms except fluor refined with anisotropic displacement parameters), the reliability factors converged to R_{obs} = 0.0417 and R_{wobs} = 0.0803 for 2549 observed reflections ($I > 2\sigma(I)$), and 81 parameters. At this stage of the refinement, the final Fourier difference map was featureless with acceptable highest (2.37 e A^{-3})

(8) Cario, L.; Kabbour, H.; Meerschaut, A. *Chem. Mater.* **2005**, *17*, 234−236.
(9) Kabbour, H.; Cario, L.; Boucher, F. *J. Mater. Chem.* **2005**, *15*, 3525−3531.
(10) Kabbour, H.; Cario, L.; Danot, M.; Meerschaut, A. *Inorg. Chem.* **2006**, *45*, 917−922.
(11) Rodríguez-Carvajal, J. *FULLPROF*; LLB: Gif-sur-Yvette Cedex, France, 2001, http://www-llb.cea.fr/fullweb/fp2k/fp2k.htm.
(12) Roisnel, T.; Rodriguez-Carvajal, J. *Mater. Sci. Forum* **2001**, *378*−*381*, 118−123.
(13) *SHELXTL*; Brucker: Madison, WI, 1998.

Table 1. Crystallographic Data, Experimental Details, and Refinement Results Presented for the Structure of $Ba_2Sb_2Se_4F_2$

Crystallographic data	
chemical formula	$Ba_2Sb_2Se_4F_2$
mol wt (g mol^{-1})	872.02
symmetry	triclinic
space group	$P\bar{1}$
a (Å)	6.1944(12)
b (Å)	6.3315(13)
c (Å)	13.804(3)
α (deg)	85.34(3)
β (deg)	85.18(3)
γ (deg)	89.82(3)
vol (Å^3)	537.7(2)
Z	2
density	5.386
cryst size (μm)	35 × 60 × 100
data collection	
temp (K)	293
wavelength (Å)	0.71073
F(000)	736
θ (deg) range	5.02−30.00
h, k, l ranges	$-8 < h < 8$ $-8 < k < 8$ $-19 < l < 19$
collected reflns	13793
independent reflns	3123
obsd reflns ($I > 2\sigma(I)$)	2549
abs correction	Analytique
abs coeff (mm^{-1})	25.697
T_{min}/T_{max}	0.3053/0.7761
R_{int}	0.0630
refinement results	
method	least-squares on F^2
F(000)	736
data/restraints/params	3123/0/81
reliability factor	$R_{obs} = 0.0417$ $R_{all} = 0.0600$
weighted reliability factor	$R_{wobs} = 0.0803$ $R_{wall} = 0.0838$
S	1.214
electronic residues (e$^-$/Å^3)	2.369/−1.563

and deepest (−1.56 e.Å^{-3}) peaks. Details on data collection and structure refinements are given in Table 1.

Theoretical Calculations

The cell and atomic position parameters of $Sr_2Sb_2Se_4F_2$ and $Ba_2Sb_2Se_4F_2$ were optimized using VASP.[14] The calculations were performed with generalized gradient approximations (GGA) using the Perdew−Wang 91[15] functional and PAW pseudopotentials.[16] The cutoff energy was 400 eV with a 7 × 7 × 2 Monkhorst−Pack[17] k-point mesh. The geometry convergence criterion chosen were the forces with $|F - \max| = 0.03$ eV/Å.

Results and Discussion

In our previous work, we have shown that the structure of $Ba_2SnS_3F_2$ resulted from the stacking of 2D building blocks of the rock salt and fluorite types.[10] In fact, as shown in Figure 1, $Ba_2SnS_3F_2$ represents the first member with $n = 0$ of a new homologous series $Ae_2M_{1+n}X_{3+n}F_2$ (Ae = Sr, Ba; M = main group metal; X = S, Se; n= integer). Using simple geometric considerations, we could indeed predict the structures of higher homologues with $n \geq 1$ from the stacking of the fluorite 2D building blocks $[Ae_2F_2]$ with rock salt 2D building blocks increasing incrementally in size with n (see Figure 1). To expand the homologous series $Ae_2M_{1+n}X_{3+n}F_2$, we looked for rock salt 2D building blocks of various sizes reported in the literature. For the $n = 1$ member, we found a suggested 2D building block, $[Sb_2Se_4]$.[18] Considering this rock salt 2D building block, we could propose that $Sr_2Sb_2Se_4F_2$, and $Ba_2Sb_2Se_4F_2$ would be possible $n = 1$ homologues. To improve the structure prediction, we have optimized the handmade structure of $Sr_2Sb_2Se_4F_2$, and $Ba_2Sb_2Se_4F_2$ using the program VASP, which allows relaxation of both the cell and atomic parameters. This calculation converged with values close to the handmade structure. Table 2 gives the cell and atomic position parameters for the optimized structure of $Sr_2Sb_2Se_4F_2$ (space group *P4/nmm*).

Table 2. Optimized Atomic Positions Parameters and Main Interatomic Distances Obtained for the Hypothetical Tetragonal Structures of $Sr_2Sb_2Se_4F_2$[a]

atom	site	x	y	z (Sr)
Ae	2c	1/4	1/4	0.6001
Sb	2c	1/4	1/4	0.1299
Se1	2c	1/4	1/4	0.3079
Se2	2c	1/4	1/4	0.8926
F	2b	3/4	1/4	1/2

	distance (Å)
Sr−F (×4)	2.504
Sb−Se1	2.553
Sb−Se2 (×4)	2.920

[a] The optimization was compatible with the space group *P4/nmm* and led to cell parameters of $a = 4.11$ Å and $c = 14.34$ Å.

We then tried to synthesize both compounds, $Sr_2Sb_2Se_4F_2$ and $Ba_2Sb_2Se_4F_2$, using a high-temperature ceramic method. For $Ba_2Sb_2Se_4F_2$, we obtained an inhomogeneous sample, but we could observe the presence of numerous crystals. These platelets, crystals with metallic luster, were analyzed and the following atomic percentages were found for Ba, Sb, and Se, respectively: 25.6(45), 24.3(6), and 50.1(5)%. Fluorine was also detected. This result is in good agreement with the theoretical values (Ba, 25%; Sb, 25%; Se, 50%) expected for $Ba_2Sb_2Se_4F_2$. The reaction product for $Sr_2Sb_2Se_4F_2$ appeared to be homogeneous. However, the powder diagrams revealed some weak peaks related to binary SrF_2 and Sb_2O_5. The presence of this very small amount of the binary oxide (less than 1%) is likely the result of a slight reaction with the silica tube or an oxidation of the starting materials. Chemical analysis of this powder sample revealed the presence of Sr, F, Sb, and Se with atomic percentages of 26.0(5), 26.5(5), and 47.5(1.0)% for Sr, Sb, and Se, respectively. These values compare reasonably well with the theoretical values (Sr, 25%; Sb, 25%; Se, 50%) expected for $Sr_2Sb_2Se_4F_2$, without consideration of the fluorine element. Both these analyses and the comparison of the experimental powder diagrams with the simulated powder diagrams obtained from the structure predictions, confirmed

(14) Kresse, G.; Furthmüller, J. *Vienna Ab Initio Simulation Package (VASP)*; Institut für Materialphysik: Wien, Austria, 2004, http://cms.mpi.univie.ac.at/vasp/vasp/vasp.
(15) Perdew, J. P.; Wang, Y. *Phys. Rev. B* **1992**, *45*, 13244.
(16) Kresse, G.; Joubert, D. *Phys. Rev. B* **1999**, *59*, 1758.
(17) Monkhorst, H. J.; Pack, J. D. *Phys. Rev. B* **1976**, *13*, 5188.
(18) Guittard, M.; Bénazeth, S.; Dugué, J.; Jaulmes, S.; Palazzi, M.; Laruelle, P.; Flahaut, J. *J. Solid State Chem.* **1984**, *51*, 227−238.

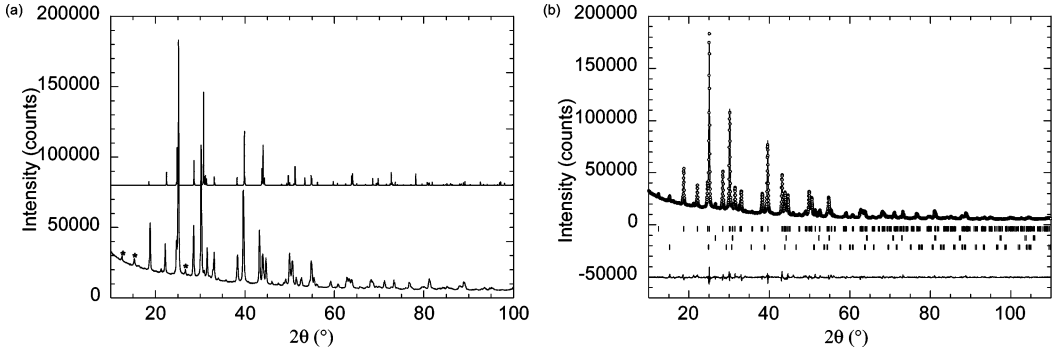

Figure 2. (a) Comparison of the observed X-ray diffraction pattern recorded for $Sr_2SbSe_4F_2$ with the pattern simulated from the structure prediction. (b) Structure of $Sr_2SbSe_4F_2$ refined using the Rietveld method: open circles represent the observed X-ray diffraction pattern and the black line represents the calculated intensities by the Rietveld method. The bottom curve is the difference between the experimental and the calculated intensities.

Table 3. Atomic Positions Parameters, Isotropic Displacement Parameters (Å^2), and Main Interatomic Distances Obtained from the Powder Structure Refinement of $Sr_2Sb_2Se_4F_2$ in the Space Group *P4/nmm* (R_{Bragg} = 4.79%, R_p = 13.76%, R_{wp} = 11.87%, and R_{exp} = 2.71%) with Cell Parameters of a = 4.1926(3) Å and c = 14.2145(13) Å

atom	x	y	z	U_{iso}
Sr	1/4	1/4	0.5968(4)	0.013(3)
Sb	1/4	1/4	0.1361(4)	0.019(2)
Se1	1/4	1/4	0.3133(4)	0.008(3)
Se2	1/4	1/4	0.8814(6)	0.045(4)
F	3/4	1/4	1/2	0.039(13)

	distance (Å)
Sr−F (×4)	2.508(1)
Sb−Se1	2.519(2)
Sb−Se2 (×4)	2.9751(3)

the formation of a quaternary compound with the expected structure (Figure 2).

The X-ray powder pattern of the almost pure sample of $Sr_2Sb_2Se_4F_2$ was then refined using the Rietveld method with a multiple-phase procedure to take into account all impurities. Starting from the predicted structures of $Sr_2Sb_2Se_4F_2$ (space group *P4/nmm*), the refinement converged to the satisfying reliability factor R_{Bragg} = 4.79% with cell parameters of a = 4.1926(3) Å and c = 14.2145(13) Å. Moreover, we could estimate the total proportion of the SrF_2 and Sb_2O_5 impurities to be lower than 2%, which indicates that $Sr_2Sb_2Se_4F_2$ was obtained with a high level of purity (more than 98%). Figure 2 shows the experimental powder pattern recorded for this compound and the best fit we obtained using FullProf. The refined atomic position parameters and isotropic displacement parameters are given in Table 3. A fairly good agreement is found between the refined and optimized cell parameters or interatomic bond lengths. A comparison of Tables 2 and 3 shows that typical errors are on the order of 1%.

The structure of $Sr_2Sb_2Se_4F_2$ is shown Figure 3. As expected, the structure results from the alternating stacking of fluorite-type $[Sr_2F_2]$ 2D building blocks with $[Sb_2Se_4]$ 2D building blocks of a distorted NaCl-type. Antimony atoms are surrounded by five selenium atoms forming a distorted square pyramid environment with two different Sb−Se distances as shown in Figure 3.

Surprisingly, our study of the X-ray diffraction pattern of the $Ba_2Sb_2Se_4F_2$ single crystals revealed a triclinic system. This was not consistent with our structural prediction using

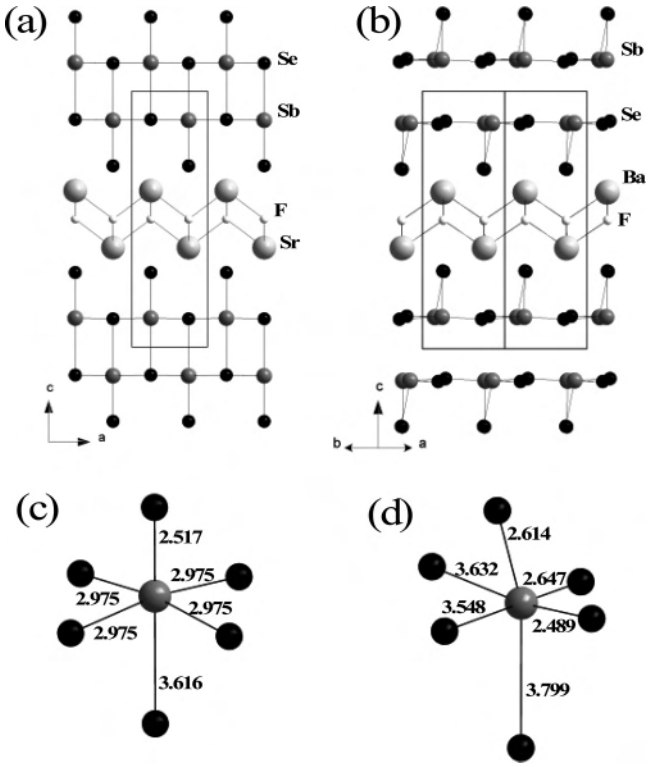

Figure 3. Representation of the structures of (a) $Sr_2SbSe_4F_2$ and (b) $Ba_2SbSe_4F_2$ projected along the 010 and 110 directions, respectively. Comparison of the Sb coordination polyhedron in both compounds, (c) $Sr_2Sb_2Se_4F_2$ and (d) $Ba_2Sb_2Se_4F_2$ with interatomic distances indicated in Å.

a quadratic system (see Table 2). However, we noticed that the measured in-plane parameters (a = 6.1944(12) Å and b = 6.3315(13) Å) and the stacking parameter (c= 13,804(3) Å) were close to the predicted values ($a_{predicted}$ = 5.94 Å and $c_{predicted}$= 14.23 Å). This strongly suggests the remaining alternation of $[Ba_2F_2]$ and $[Sb_2Se_4]$ 2D building blocks. The refinement confirmed this assumption and led to satisfying reliability factors R_{obs} = 4.17% for 2549 observed reflections (see Table 1). The obtained atomic coordinates and equivalent isotropic displacement parameters are listed in Table 4. The structure of $Ba_2Sb_2Se_4F_2$ projected along the (110) direction is shown in Figure 3. This representation highlights the distortion of the $[Sb_2Se_4]$ 2D building blocks found in $Ba_2Sb_2Se_4F_2$ compared to the one in $Sr_2Sb_2Se_4F_2$. Figure 3 also gives a comparison of the Sb coordination polyhedron

Table 4. Atomic Coordinates and Equivalent Isotropic Displacement Parameters (Å^2) Obtained from the Single Crystal Structure Refinement of $Ba_2Sb_2Se_4F_2$

atom	site	*x*	*y*	*z*	$U_{(isoeq*)}$ (Å^2)
Ba1	2i	0.2722(1)	0.5239(1)	0.3911(1)	0.0099(1)*
Ba2	2i	−0.2278(1)	1.0159(1)	0.3922(1)	0.0094(1)*
Sb1	2i	−0.2268(1)	0.6224(1)	0.1231(1)	0.0152(1)*
Sb2	2i	0.2676(1)	0.0315(1)	0.1240(1)	0.0143(1)*
Se1	2i	−0.2117(2)	0.5294(1)	0.3009(1)	0.0135(2)*
Se2	2i	0.2894(2)	0.0430(1)	0.3027(1)	0.0126(2)*
Se3	2i	−0.1602(2)	1.0300(2)	0.1269(1)	0.0175(2)*
Se4	2i	0.3478(2)	0.6276(2)	0.1153(1)	0.0208(2)*
F1	2i	−0.0004(9)	0.7468(8)	0.5017(4)	0.0117(10)
F2	2i	0.5006(9)	0.7500(8)	0.5016(4)	0.0121(10)

Table 5. Interatomic Distances (Å) Obtained from the Single Crystal Structure Refinement of $Ba_2Sb_2Se_4F_2$

Ba1−F1	2.660(6)	Sb1−Se1	2.4860(13)
Ba1−F2	2.665(5)	Sb1−Se3	2.6208(13)
Ba1−F2	2.666(5)	Sb1−Se4	2.6464(14)
Ba1−F1	2.674(5)	Sb2−Se2	2.4888(13)
Ba2−F1	2.663(5)	Sb2−Se4	2.6138(13)
Ba2−F1	2.668(5)	Sb2−Se3	2.6470(13)
Ba2−F2	2.669(6)		
Ba2−F2	2.669(6)		

in both compounds $Sr_2Sb_2Se_4F_2$, and $Ba_2Sb_2Se_4F_2$. While, in $Sr_2Sb_2Se_4F_2$, the antimony atoms are located in distorted square pyramids of Se atoms, in $Ba_2Sb_2Se_4F_2$, the antimony atoms adopt a different coordination with only three Se atoms as nearest neighbors. This is a well-known coordination in antimony compounds showing a clear signature of the lone-pair activity.[19] The same type of distortion of the $[Sb_2S_4]$ 2D building blocks was already encountered in the Franckeite misfit layered compounds.[20,21] In $Sr_2Sb_2Se_4F_2$, the lattice contraction allowed by the lower ionic radius of the Sr atoms compared to that of the Ba atoms seems to compete with the lone-pair activity and prevent this distortion.

Taking into account the structure of the Franckeite, it would have been possible to envision the structure distortion of the $[Sb_2Se_4]$ module in $Ba_2Sb_2Se_4F_2$. We have therefore made new structure optimizations for $Ba_2Sb_2Se_4F_2$ starting either from our experimental result or from a distorted quadratic structure obtained by shifting the cell angles from 90°. As expected, both calculations converged with lower energies, and the best solution was very close to the experimental result. Consequently, starting from the quadratic structure, we reached a local minimum in the surface energy, which clearly demonstrates that simulated heat methods would be highly desirable to go through local minima and reach the most stable structure.

Conclusions

In conclusion, we have succeeded in enlarging the new homologous series $Ae_2M_{1+n}X_{3+n}F_2$ (Ae = Sr, Ba; M = main group metal; n= integer) built up from the stacking of 2D building blocks of the rock salt and fluorite types. By increasing the size of the rock salt 2D building blocks, we have obtained two new $n = 1$ members of this homologous series. While $Sr_2Sb_2Se_4F_2$ compares very well with our structure optimization using VASP, the structure of $Ba_2Sb_2Se_4F_2$ shows a significant distortion with a clear signature of the lone -pair activity of antimony.

This work clearly shows that combining the use of 2D modules with phase homologies provides a powerful tool for designing new solid-state compounds. Since we have recently designed new compounds with perovskite[22] and anti-fluorite [9] 2D modules, we are currently looking for new homologous series built from these modules.

Acknowledgment. Yves Moëlo is thanked for fruitful discussions.

Supporting Information Available: Crystallographic data in CIF format. This material is available free of charge via the Internet at http://pubs.acs.org.

IC051969X

(19) Olivier-Fourcade, J.; Ibanez, A.; Jumas, J. C.; Maurin, M.; Lefebvre, I.; Lippens, P.; Lannoo, M.; Allan, G. *J. Solid State Chem.* **1990**, *87*, 366−377.

(20) Lafond, A.; Meerschaut, A.; Moëlo, Y.; Rouxel, J. *C. R. Acad. Sci. Paris* **1996**, *322*, 165−173.

(21) Bengel, H.; Jobic, S.; Moëlo, Y.; Lafond, A.; Rouxel, J.; Seo, D.-K.; Whangbo, M.-H. *J. Solid State Chem.* **2000**, *149*, 370−377.

(22) Cario, L.; Lafond, A.; Morvan, T.; Kabbour, H.; Deudon, C.; André, G.; Palvadeau, P. *Solid State Sci.* **2005**, *7*, 936−944.